Reports on Geodesy and Geoinformatics, 2022, Vol. 114, pp. 1–7

DOI: 10.2478/rgg-2022-0004
Received: 6 August 2022 / Accepted: 21 September 2022
Published online: 25 October 2022

ORIGINAL ARTICLE

A crossvalidation-based comparison of kriging and IDW in local GNSS/levelling quasigeoid modelling

Marcin Ligas [1*], Blazej Lucki [1] and Piotr Banasik [1]

[1]Department of Integrated Geodesy and Cartography, Faculty of Geo-Data Science, Geodesy and Environmental Engineering, AGH University of Science and Technology, al. Mickiewicza 30, 30-059 Kraków, Poland

[*]ligas@agh.edu.pl

Abstract

This study compares two interpolation methods in the problem of a local GNSS/levelling (quasi) geoid modelling. It uses raw data, no global geopotential model is involved. The methods differ as to the complexity of modelling procedure and theoretical background, they are ordinary kriging/least-squares collocation with constant trend and inverse distance weighting (IDW). The comparison itself was done through leave-one-out and random (Monte Carlo) cross-validation. Ordinary kriging and IDW performance was tested with a local (using limited number of data) and global (using all available data) neighbourhoods using various planar covariance function models in case of kriging and various exponents (power parameter) in case of IDW. For the study area both methods assure an overall accuracy level, measured by mean absolute error, root mean square error and median absolute error, of less than 1 cm. Although the method of IDW is much simpler, a suitably selected parameters (also trend removal) may contribute to differences between methods that are virtually negligible (fraction of a millimetre).

Key words: quasigeoid, kriging, least squares collocation, IDW, conversion surface, cross-validation

1 Introduction

In general, Global Navigation Satellite Systems (GNSS) provide 3D position (x, y, z) of any point on or above the Earth in Earth-Centered, Earth-Fixed system and it is the native system in which GNSS coordinates are delivered. Since 3D Cartesian coordinates are impractical on a surveying daily basis they are converted to geodetic coordinates: latitude, longitude and ellipsoidal height, traditionally denoted as (φ, λ, h). The latter mentioned is still problematic due to its purely geometric character related with adopted ellipsoidal model of the Earth. Hence, GNSS-based heights are not consistent with physical heights and require conversion in a valid height system, e.g., orthometric or normal (Hofmann-Wellenhof and Moritz, 2006).

Through the years many interpolation methods have been involved in generating conversion surfaces (in local and regional scales) enabling transition between geometric and physical heights, e.g., polynomial regression (Borowski and Banaś, 2019; Gucek and Bašić, 2009; Kim et al., 2018; Zhong, 1997), neural networks (Akyilmaz et al., 2009; Kaloop et al., 2021), geographically weighted regression (Dawod and Abdel-Aziz, 2020), kriging (Ligas and Szombara, 2018; Orejuela et al., 2021), least-squares collocation (LSC) (You, 2006), Inverse Distance Weighting (IDW) (Radanović and Bašić, 2018) to mention only a few. Very often, conversion surfaces take the form of corrector surfaces due to the use of global geopotential models or gravimetric models generated prior to eliminating inconsistencies by fitting to GNSS/levelling data (Elshambaky, 2018; You, 2006).

This study uses ordinary kriging which is identical to least squares collocation with constant trend (Ligas, 2022; Schaffrin, 2001) and may be described by two acronyms: BLUE (Best Linear Unbiased Estimation) and BLUP (Best Linear Unbiased Prediction). BLUE concerns the estimation of a fixed effect (unknown expected value) and BLUP prediction of a random effect (signal or signal+noise). The spine of two methods is a structure function (covariance or semivariance) that captures spatial continuity and variability of the data (random field being a representation of the analysed phenomena). IDW is a simple deterministic interpolation

Publisher: De Gruyter

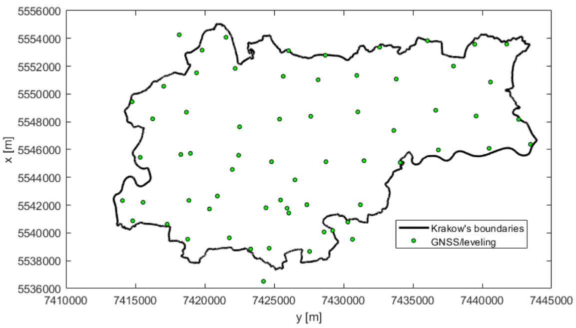

Figure 1. Spatial distribution of GNSS/leveling points (x, y in EPSG:2178)

method relying on an a priori assumption of decreasing weights with a distance from the target point (Babak and Deutsch, 2009).

The goal of this study is to compare these two methods differing in complexity of theory and computational effort and should not be directly connected to the one of Banasik et al. (2020) which was a kind of quasi-geoid model development report. The comparison itself is made in cross-validation mode with varying steering parameters of the methods, i.e., structure function and number of nearest neighbours in case of kriging/LSC, and power parameter (exponent) and number of nearest neighbours in case of IDW.

2 Study area and data used

Study area covers the city of Krakow in the south-eastern part of Poland and is spread over approximately 20 km x 30 km. In order to validate the effectiveness of kriging/LSC and IDW preceded by 1^{st} and 2^{nd} degree polynomial trend removal, 66 GNSS/levelling points were used. No points were excluded from the analysis. PL-ETRF2000 and PL-EVRF2007-NH are used for ellipsoidal and normal heights; respectively. Planar cartesian coordinates $[x, y]$ expressed in PL-2000/7 coordinate system (EPSG:2178). Spatial distribution of the GNSS/levelling points used for modelling purposes is shown in Figure 1. Details as to GNSS and leveling measurements and accuracy issues are reported in Banasik et al. (2020).

3 Generation of local quasi-geoid models, methods, and their validation

3.1 General methodology of local quasi-geoid models construction

The study uses GNSS-derived ellipsoidal and levelled normal heights, without the use of external data like a gravimetric geoid model or a global geopotential model, to integrate them through a local conversion surface modelling. In general, the local conversion surfaces may be expressed by:

$$\zeta = h - H^N = \mu(\upsilon) + \delta(\upsilon) \tag{1}$$

where ζ is a height anomaly, h stands for an ellipsoidal height (GNSS-based), H^N is a normal height (levelling-based), μ is a trend, δ is a disturbance (potentially spatially correlated) and $\upsilon = [x, y]$ stands for a position.

In this contribution, kriging/least squares collocation and a simple distance-based interpolation method, i.e., inverse distance weighting have been used. Also, a polynomial trend surface fitting approach was adopted since it is the most obvious and the most common way of approximating spatially varying phenomena (Borowski and Banasik, 2020; Tusat and Mikailsoy, 2018). It was used in combination with the methods mentioned above and played a role of a long wavelength component in height anomalies. IDW was chosen due to its simplicity. Kriging (LSC), which is decidedly more complex than IDW, was used since it has a grounded position in different spatial interpolation problems. In both kriging and IDW, the trend models in Equation (1) were modelled by simple polynomial surfaces of low degree (1^{st} and 2^{nd}), namely:

$$\mu(\upsilon) = \beta_0 + \beta_1 x + \beta_2 y \tag{2}$$

$$\mu(\upsilon) = \beta_0 + \beta_1 x + \beta_2 y + \beta_3 xy + \beta_4 x^2 + \beta_5 y^2 \tag{3}$$

and their reduced versions resulting from eliminating parameters β that were not statistically significant. The models were fit with the least squares method. Whilst developing the approximation function a mapping of the spatial domain onto a unit square has been used according to the formulas (to avoid possible numerical problems):

$$X_i = \frac{x_i - x_{min}}{x_{max} - x_{min}} \qquad Y_i = \frac{y_i - y_{min}}{y_{max} - y_{min}} \tag{4}$$

where x_{min}, x_{max}, y_{min}, y_{max} stand for extreme values of coordinates for a bounding rectangle.

The goal of the study was to examine whether the method like kriging (LSC) may substantially outperform IDW in the local height anomaly field modelling problem. The study addresses also a question whether the use of a global neighbourhood (all available data) provides any improvement over a local neighbourhood (limited number of data) in the modelling procedure. In the case of IDW, the conducted tests were also to check whether commonly used exponent value equal to 2 is always justifiable. The methods were exhaustively tested, as to the predictive capability of the model (out-of-sample), in two variants of cross-validation technique: leave-one-out (LOOCV) and random (Monte Carlo, MCCV). The first mentioned rests on a sequential removal of a single observation from a dataset, predicting its value on the basis of the model built from the remaining data and a comparison of the predicted value with the reference value previously removed. The second variant rests on a random removal of a given percentage of observations from the data set (20% adopted in this study, 14 points), forecasting their values on the basis of the model built from the remaining data and comparison with reference values (previously removed) and such a procedure is repeated n-times (1000 repetitions adopted in this study). This way of testing gives the accuracy characteristics of the prediction model and, in fact, plays two roles. Firstly, it helps to select optimal steering parameters within a given approach, here, in both IDW (number of nearest neighbours, power parameter) and kriging (number of nearest neighbours, semivariogram model). Secondly, it gives the answer which approach could claim to be the best among examined as far as accuracy characteristics are considered. It also allows to assess the stability of the adopted model, i.e., how the change of steering parameters impacts the results. In both cross-validation variants the root mean square, mean absolute, median absolute cross-validation errors were used. All the above mentioned characteristics are based on the differences between the observed values (removed) and the corresponding model-based predicted values.

3.2 Kriging/Least squares collocation

Kriging is a large family of univariate and multivariate linear and nonlinear predictors within geostatistics – discipline that has its roots in mining and geology and statistical methods used therein. In its linear form it is equivalent to LSC (Ligas, 2022; Schaffrin, 2001) that is characterized as an advanced method that combines adjustment, filtering and prediction in one computational procedure (Moritz, 1972). The backbone of the methods is a structure function of a random field that is a representation of a phenomenon under study. In the LSC the covariance function (second-order stationarity) plays a key role, on the other hand, in geostatistics it is the semivariance function (intrinsic stationarity). The two structure functions are equivalent under the second-order stationarity, namely:

$$C(d) = C(0) - \gamma(d) = \left(\sigma_n^2 + \sigma_s^2\right) - \gamma(d) \tag{5}$$

where: ${\sigma_n}^2$ is a variance of noise (nugget effect), ${\sigma_s}^2$ is a variance of a signal (partial sill), d is a distance.

Since the least-squares collocation method is better known within the geodetic community, this study adopts geostatistical terminology. In both methods a random function (or simply the data) may be decomposed into trend, signal and noise, what may be expressed as (the 2nd row concerns a single point prediction):

$$\begin{matrix}\text{observed} \\ \text{predicted}\end{matrix} \begin{cases} \mathbf{Z}(\upsilon) = \mu(\upsilon) + \mathbf{s}(\upsilon) + \epsilon(\upsilon) = trend + signal + noise \\ S(\upsilon_0) = \mu(\upsilon_0) + s(\upsilon_0) = trend + signal \end{cases} \tag{6}$$

where $\mathbf{Z}$ stands for observed data, μ is a trend model, either a function of a position in space or a constant, $\mathbf{s}$ is a random signal, ϵ stands for noise, υ stands for a position in space, here planar coordinates $\upsilon = [x, y]$.

The most widely form of kriging, i.e., ordinary kriging (Wackernagel, 2003) is used in this contribution. Ordinary kriging is optimal in the sense of BLUP if the mean value of a random function is an unknown constant (Cressie, 1993). It is identical to least-squares collocation with parameters (Ligas, 2022; Schaffrin, 2001) where the trend is modelled as an unknown constant. In this case the following stochastic characteristics holds (denotation of location υ will be omitted):

- Expected value of either signal or noise is zero:

$$E(\epsilon) = E(\mathbf{s}) = \mathbf{0}, \quad E(s_0) = 0; \tag{7}$$

- Signal and noise are uncorrelated:

$$E\left(\mathbf{s}\epsilon^T\right) = E\left(\epsilon\mathbf{s}^T\right) = \mathbf{0} \tag{8}$$

Covariance matrix of sample disturbances (also observations – observations or data – data) which is the sum of a covariance matrix of the signal $\mathbf{\Omega_{ss}}$ and a covariance matrix of noise $\mathbf{\Omega}_{\epsilon\epsilon}$ is given by:

$$E\left[(\mathbf{s}+\epsilon)(\mathbf{s}+\epsilon)^T\right] = E\left(\mathbf{s}\mathbf{s}^T\right) + E\left(\epsilon\epsilon^T\right) = \mathbf{\Omega_{ss}} + \mathbf{\Omega}_{\epsilon\epsilon} = \mathbf{\Omega_{ZZ}} \tag{9}$$

Cross – covariance vector between sample signal and prediction signal (or observations – prediction signal) reads:

$$E\left[(\mathbf{s}+\epsilon)s_0^T\right] = E\left(\mathbf{s}s_0^T\right) + E\left(\epsilon s_0^T\right) = E\left(\mathbf{s}s_0^T\right) = E\left(\mathbf{Z}s_0^T\right) = \omega_{\mathbf{s}s_0} = \omega_{\mathbf{Z}s_0} \tag{10}$$

and a signal variance:

$$E\left(s_0 s_0^T\right) = E\left(s_0^2\right) = E\left(s^2\right) = \sigma_s^2 \tag{11}$$

Having in mind the above characteristic the ordinary (filtered) kriging predictor (or least-squares collocation with an unknown constant trend) may be expressed as:

$$\hat{S}_0 = \hat{\mu} + \omega_{\mathbf{s}s_0}^T \mathbf{\Omega_{ZZ}^{-1}} (\mathbf{Z} - \mathbf{u}\hat{\mu}) \tag{12}$$

where the unknown constant mean value is estimated via generalized least squares:

$$\hat{\mu} = \left(\mathbf{u}^T \mathbf{\Omega_{ZZ}^{-1}} \mathbf{u}\right)^{-1} \mathbf{u}^T \mathbf{\Omega_{ZZ}^{-1}} \mathbf{Z} \tag{13}$$

and $\mathbf{u}$ is a vector of ones.

The quality of prediction is measured through the prediction variance:

$$\begin{aligned} \sigma_{OFK}^2 &= \sigma_S^2 - \omega_{\mathbf{s}s_0}^T \mathbf{\Omega_{ZZ}^{-1}} \omega_{\mathbf{s}s_0} + \\ &+ \left(1 - \omega_{\mathbf{s}s_0}^T \mathbf{\Omega_{ZZ}^{-1}} \mathbf{u}\right) \left(\mathbf{u}^T \mathbf{\Omega_{ZZ}^{-1}} \mathbf{u}\right)^{-1} \left(1 - \omega_{\mathbf{s}s_0}^T \mathbf{\Omega_{ZZ}^{-1}} \mathbf{u}\right)^T \end{aligned} \tag{14}$$

All mentioned covariance vectors and matrices are constructed on the basis of covariance functions and this study uses the following ones:

- Rational quadratic model or generalized Cauchy/Hirvonen model (Chiles and Delfiner, 1999; Meier, 1981):

$$C\left(d, \sigma_n^2, \sigma_s^2, r\right) = \begin{cases} \sigma_n^2 + \sigma_s^2 & d = 0 \\ \dfrac{\sigma_s^2}{\left[1 + \left(\frac{d}{r}\right)^2\right]^{\alpha}} & d > 0 \end{cases} \tag{15}$$

  where: $\alpha > 0$, for $\alpha = 1$ one obtains the Cauchy (Ohio) model (Jordan, 1972), for $\alpha = 1/2$ the Moritz model, and for $\alpha = 3/2$ the Poisson model (Meier, 1981);
- Markov's 2nd (Equation 16) and Markov's 3rd (Equation 17) order model (Radon transform of order 2 and 4 of the exponential model) (Chiles and Delfiner, 1999; Jordan, 1972):

$$C\left(d, \sigma_n^2, \sigma_s^2, r\right) = \begin{cases} \sigma_n^2 + \sigma_s^2 & d = 0 \\ \sigma_s^2 \left(1 + \frac{d}{r}\right) e^{-\left(\frac{d}{r}\right)} & d > 0 \end{cases} \tag{16}$$

$$C\left(d, \sigma_n^2, \sigma_s^2, r\right) = \begin{cases} \sigma_n^2 + \sigma_s^2 & d = 0 \\ \sigma_s^2 \left(1 + \frac{d}{r} + \frac{d^2}{3r^2}\right) e^{-\left(\frac{d}{r}\right)} & d > 0 \end{cases} \tag{17}$$

As may be seen, all the above models are supplemented by a nugget effect structure. In fact, the mentioned nugget effect has a broader meaning than only a noise variance since it encompasses also a microscale variation due to lack of knowledge of a process behaviour at distances shorter than minimum distance between observations.

3.3 Inverse distance weighting (IDW) interpolation method

Inverse distance interpolation is a widely used technique mainly due to its conceptual and numerical simplicity. In fact, it belongs to a broader class of spatial interpolation distance-decay models (e.g., exponential or Gaussian). The computational formula of IDW method is simply a weighted average of neighbouring values, assigning larger weights to closer points (underlying assumption of spatial autocorrelation), and it reads:

$$\hat{Z}_0 = \lambda^T \mathbf{Z} = \lambda_1 Z_1 + \lambda_2 Z_2 + \ldots + \lambda_n Z_n \tag{18}$$

with:

$$\lambda_i = \frac{d_{0i}^{-\alpha}}{\sum\limits_{j=1}^{n} d_{0j}^{-\alpha}} (i = 1..n) \tag{19}$$

where subscript '0' refers to the point being predicted, n is a number of points from an adopted neighbourhood, α is a power parameter.

Although the most common value of α in Equation (19) is 2, perhaps due to the analogy with the gravitational force model, there is no particular explanation for this value. Since there is no exact recommendation about the choice of exponent and the optimal number of neighbouring points (Babak and Deutsch, 2009), therefore, in this study, the leave-one-out and random crossvalidation were used to assist in finding the parameters. During the search the following values for the power parameter and number of neighbours were used: α = 1...5 with a step 0.5 and n = 3...N with a step 1, where N denotes all available data.

4 Results

In order to compare considered interpolation (prediction) methods and their steering parameters impact on final results the leave-one-out and random crossvalidation procedures, described before, were applied. The following synthetic indicators of interpolation quality, measured through crossvalidation technique, were used:

- Mean Absolute Error (MAE):

$$MAE = \frac{1}{n}\sum_{i=1}^{n} |e_i| ; \tag{20}$$

- Root Mean Square Error (RMSE):

$$RMSE = \sqrt{\frac{1}{n}\sum_{i=1}^{n} e_i^2} ; \tag{21}$$

- Median Absolute Error (MeAE):

$$MeAE = med\,|e_i| \tag{22}$$

where e is a crossvalidation prediction error, i.e., the difference between observed ζ_i^O (previously removed) and corresponding predicted height anomaly ζ_i^P:

$$e_i = \zeta_i^O - \zeta_i^P \tag{23}$$

The three measures were used to confirm or deny the repeatability of general tendency that a given set of steering parameters of a method is superior to another.

Both Kriging/LSC and IDW were applied to residuals obtained after 1st and 2nd degree polynomial trend surface removal. Analysis of ordinary kriging (or LSC with a constant trend) and IDW performance was tested with a local (using limited number of data) and global (using all available data) neighbourhoods using various planar covariance function models in case of kriging and various exponents in case of IDW. In order to find the optimal parameters for considered dataset the following procedure was implemented:

In case of kriging/LSC:
Loops were run through all adopted covariance functions (computed once for the entire dataset) and number of neighbours varying from 3 to n with the step of 1 neighbour, where n denotes all available data. Each time accuracy characteristics of LOOCV and MCCV were computed. In LOOCV this simulation gives 315 "bulk" predictions of 66 points (or 20790 single point predictions) for the adopted trend surface. In case of two trend surfaces the numbers double. In MCCV the simulation gives 250 "bulk" predictions of 14 points (or 3500 single point predictions) for the adopted trend surface in a single trial. Since the overall number of random trials was 1000 this gives 250 000 "bulk" predictions (3 500 000 single predictions). In case of two trend surfaces the numbers double. Partial results concerning only one of the best performing structure function, the Poisson model, are presented in Figures 2 and 3. It is worth mentioning that, in overall, the entire family of rational quadratic models performed better than Markov's models for this dataset. Table 1 lists averaged (of all cases of the number of neighbours) MAE, RMSE and MeAE for a given structure function to give the synthesized insight into the results.

Table 1. Averaged MAE, RMSE, MeAE for a given structure function

Structure function	MAE [mm]	RMSE [mm]	MeAE [mm]
Rational Quadratic α = 1	6.6	8.3	5.2
Rational Quadratic α = 1/2	6.7	8.3	6.0
Rational Quadratic α = 3/2	6.6	8.4	5.1
Markov's 2nd	7.0	8.6	6.0
Markov's 3rd	7.5	9.4	5.8

In case of IDW:
Loops were run through exponents α varying from 1 to 5 with 0.5 increment and number of neighbours varying from 3 to n with the step of 1 neighbour, where n denotes all available data. Each time LOOCV and MCCV accuracy characteristics were computed. Due to the large number of results, only the most relevant are presented in Figures 4 – 7. In LOOCV this simulation gives 567 "bulk" predictions of 66 points (or 37422 single point predictions) for the adopted trend surface. In case of two trend surfaces the numbers double. In MCCV the simulation gives 450 "bulk" predictions of 14 points (or 6300 single point predictions) for the adopted trend surface in a single trial. Since the overall number of random trials was 1000 this gives 450 000 "bulk" predictions (6 300 000 single predictions). In case of two trend surfaces the numbers double.

The numbers above give an idea of the number of predictions performed to estimate the accuracy of the two methods and generate a kind of confidence to the results obtained for this dataset.

Figure 2 confronts the results of kriging's based LOOCV (Fig. 2a) and MCCV (Fig. 2b) after removal of 1st degree polynomial trend surface for the Poisson covariance function with varying neighbourhood size. Adopted quality measures MAE, RMSE, MeAE are slightly higher (~ 0.5 mm) for MCCV but this simply results from the removal of 20% of data (14 points) from the entire dataset. Also, plots of these statistics seem to be smoother but this results from averaging from 1000 repetitions of data random removal. In fact, this negligible difference confirms stability of this approach. It is visible (mainly for the LOOCV) that the exhaustive neighbourhood is not necessary to obtain satisfactory (or even best) results. Here, we notice that this occurs for something in between 10 – 15 nearest neighbours (but the difference is a fraction of a millimeter).

Figure 3 shows the same statistics with detrending by means of 2nd degree trend surface model. Statistics are slightly higher than previously what indicates that, for this dataset, the structure hidden in residuals, generated after detrending, is better captured for the lower degree polynomial model. This shows that increasing trend surface degree is not always justifiable. The overall behavior of accuracy measures is similar, i.e., stabilization of values for increasing number of neighbours and some evidence that the nearest observations may be enough to obtain satisfactory results.

On the other hand, since the removal of quadratic trend surface turned out to be adequate for IDW method, and due to large number of outcomes in this analysis (impossible to show all the statistics on a single chart without missing readability) only abbreviated results will be presented (showing all of them would take a lot of space and would not contribute to a better insight into the problem).

Figure 4 shows MAEs for the entire range of nearest neighbours (3 – 65) and exponents (1 – 5) in leave-one-out crossvalidation. The highest variability of this statistic is visible for the range of 3 – 15 neighbours, then it stabilizes, except for exponents 1, 1.5, and 2 for which MAEs continue to grow up to ~30 neighbours (the same holds for remaining statistics). The latter mentioned exponents characterize themselves with the highest MAE in overall, remaining ones stay roughly on the same level in the entire range of neighbours. Since Figure 3 is hard to read for small number of neighbours, the Figures 5 – 7 presenting MAE, RMSE and MeAE obtained from LOOCV are limited to 15 nearest neighbours.

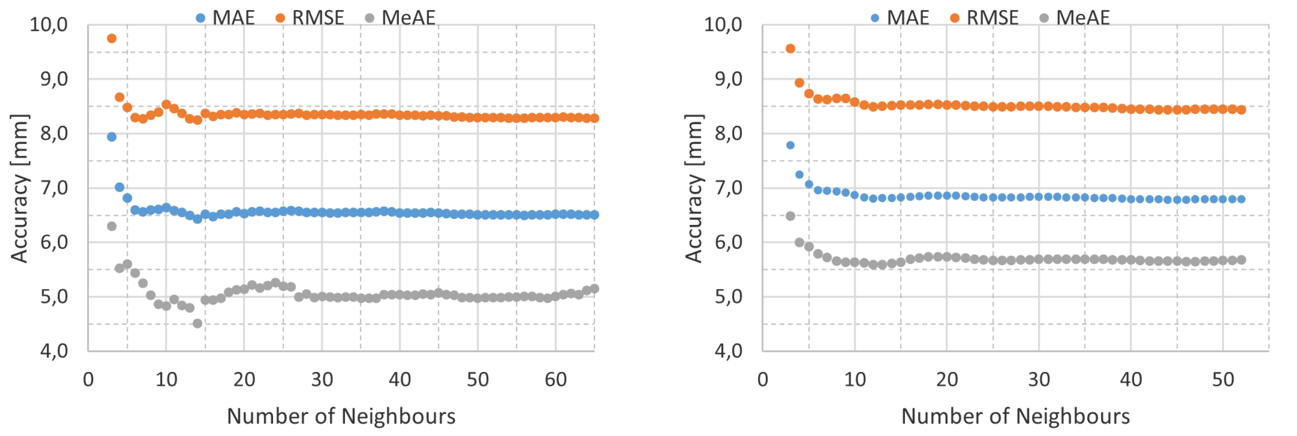

(a) Leave-one-out crossvalidation

(b) Random crossvalidation

Figure 2. Leave-one-out crossvalidation (a) and random crossvalidation (b) accuracy characteristics (MAE, RMSE, MeAE) with respect to the number of neighbours for ordinary kriging with rational quadratic α = 3/2 (Poisson) semivariogram model after removal of planar trend

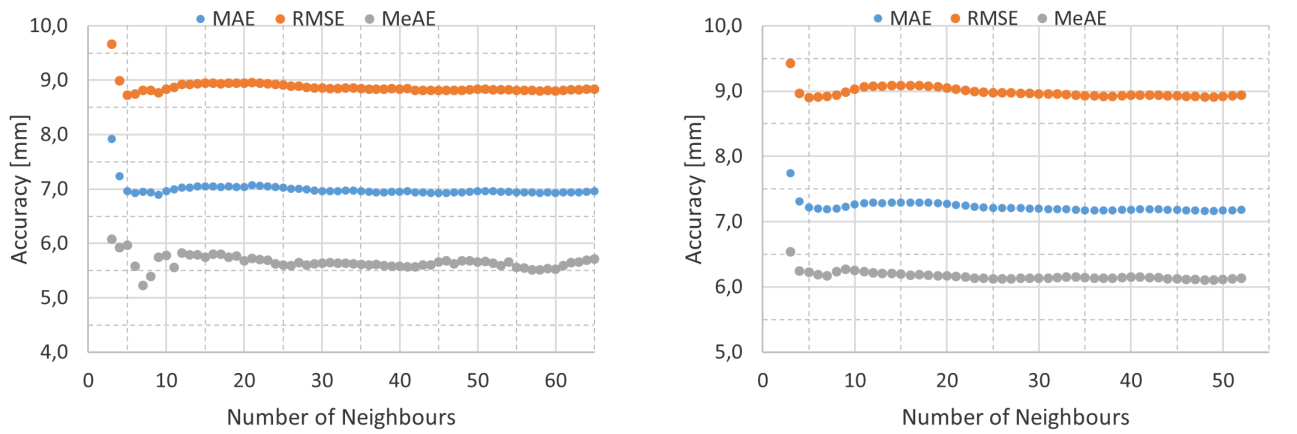

(a) Leave-one-out crossvalidation

(b) Random crossvalidation

Figure 3. Leave-one-out crossvalidation (a) and random crossvalidation (b) accuracy characteristics (MAE, RMSE, MeAE) with respect to the number of neighbours for ordinary kriging with rational quadratic α = 3/2 (Poisson) semivariogram model after removal of quadratic trend

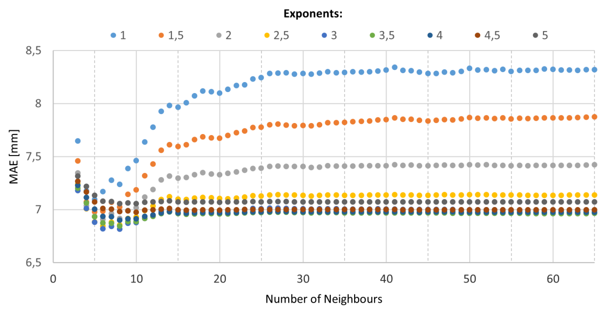

Figure 4. MAE from LOOCV with respect to the number of neighbours (3 – 65, full range) for IDW with exponents varying from 1 to 5 with 0.5 increment after removal of quadratic trend model

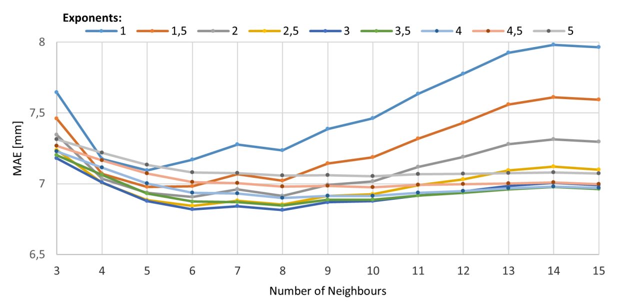

Figure 5. MAE from LOOCV with respect to limited number of neighbours for IDW

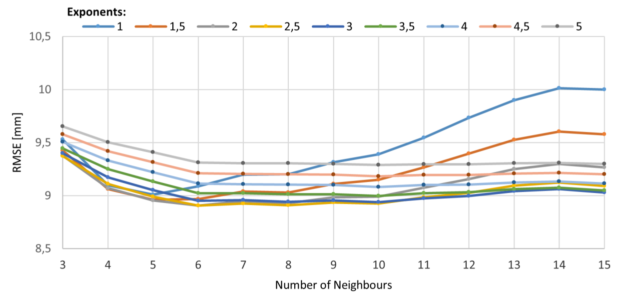

Figure 6. RMSE from LOOCV with respect to limited number of neighbours for IDW

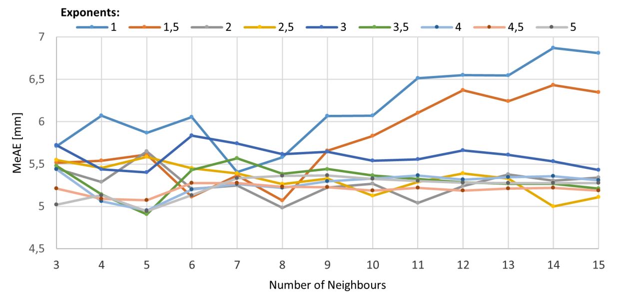

Figure 7. MeAE from LOOCV with respect to limited number of neighbours for IDW

In general, the Figures show the lowest values of the quality statistics for app. 5 – 10 nearest neighbours. The differences between exponents are not significant from practical viewpoint (maximum discrepancy less than 0.5 mm) except for exponents 1, 1.5 and 2 for MAE and 1, 1.5 for RMSE and MeAE where upward tendency is visible (differences ~1 mm). Other exponents keep stability within shown range of neighbours. It clearly shows that this kind of analysis assists in selecting the proper exponent and number of nearest neighbours necessary in order to obtain optimal results for a given dataset. Accuracy statistics for LOOCV in case of planar trend removal are app. 1 – 1.5 mm higher. Since IDW does not provide an internal measure of interpolation quality the results of crossvalidation may be adopted as a global measure of IDW performance for a given set of parameters. As in kriging, due to the same reasons, adopted quality characteristics in random crossvalidation were slightly higher ~1 mm for both cases of trend removal. It is also worth noting that these results do not deviate much from those obtained from kriging. The best results for IDW measured by means of MAE are for 6, 8 nearest neighbours, exponents 3.5, 3, 2.5 and they are on the level of 6.8 mm. In case of ordinary kriging the best results measured by MAE are for 14 nearest neighbours and are on the level of 6.4 mm. The remaining statistics are 0.5 – 0.8 mm higher for IDW than for kriging when mentioned configuration of parameters is involved.

5 Conclusions

In this study, two methods of spatial prediction (interpolation) with varying degree of complexity have been applied and compared in the problem of a local (small-area) quasigeoid conversion surface modelling. The study showed no practical difference between results of kriging/LSC and suitably chosen parameters for IDW interpolation for analysed dataset. However the intra (within a method) and inter (between methods) differences in the entire range of steering parameters may be significant. Both methods have their advantages and disadvantages.

The main advantage of kriging/LSC is that the entire prediction procedure is consistent in the sense that it results from strict reasoning without a heuristic element. It also takes into account the spatial structure of the data through modelling either a covariance function or a semivariance function. But since the latter mentioned are inferred from the data, in fact, their empirical and analytical form are analyst's experience dependent. In addition, it provides a prediction variance that is a measure of prediction quality.

On the other hand, IDW has an advantage over kriging/LSC since it does not require solving any system of equations for the weights because it rests on a priori assumption of change of weights with distance-decay. But as shown in this contribution, selection of optimal distance-decay exponent and number of neighbours is not straightforward. It is easy to automatize. In general, it does not provide a measure of interpolation quality.

The applied crossvalidation technique balances the advantages and disadvantages of the methods since it assists in selecting optimal parameters for a given dataset and provides measures of crossvalidation accuracy which may be accepted as a final measure of model quality. The findings from this study show that a conversion surface which compensate the inconsistency between the different types of heights with the average accuracy of less than 1 cm is achievable with the use of both tested methods.

Acknowledgements

The paper is a result of research on geospatial methods carried out within statutory research no. 16.16.150.545 at the Department of Integrated Geodesy and Cartography, AGH University of Science and Technology, Krakow.

References

Akyilmaz, O., Özlüdemir, M., Ayan, T., and Çelik, R. (2009). Soft computing methods for geoidal height transformation. *Earth, planets and space*, 61(7):825–833, doi:10.1186/BF03353193.

Babak, O. and Deutsch, C. V. (2009). Statistical approach to inverse distance interpolation. *Stochastic Environmental Research and Risk Assessment*, 23(5):543–553.

Banasik, P., Bujakowski, K., Kudrys, J., and Ligas, M. (2020). Development of a precise local quasigeoid model for the city of Krakow – QuasigeoidKR2019. *Reports on Geodesy and Geoinformatics*, 109(1):25–31, doi:10.2478/rgg-2020-0004.

Borowski, Ł. and Banaś, M. (2019). The best robust estimation method to determine local surface. *Baltic Journal of Modern Computing*, 7(4):525–540, doi:10.22364/bjmc.2019.7.4.06.

Borowski, Ł. and Banasik, P. (2020). The conversion of heights of the benchmarks of the detailed vertical reference network into the PL-EVRF2007-NH frame. *Reports on geodesy and geoinformatics*, 109(1):1–7, doi:10.2478/rgg-2020-0001.

Chiles, J.-P. and Delfiner, P. (1999). *Geostatistics: modeling spatial uncertainty*. John Wiley & Sons.

Cressie, N. (1993). *Statistics for spatial data*. John Wiley & Sons.

Dawod, G. M. and Abdel-Aziz, T. M. (2020). Utilization of geographically weighted regression for geoid modelling in Egypt. *Journal of Applied Geodesy*, 14(1):1–12, doi:10.1515/jag-2019-0009.

Elshambaky, H. T. (2018). Application of neural network technique to determine a corrector surface for global geopotential model using GPS/levelling measurements in Egypt. *Journal of Applied Geodesy*, 12(1):29–43, doi:10.1515/jag-2017-0017.

Gucek, M. and Bašić, T. (2009). Height transformation models from ellipsoidal into the normal orthometric height system for the territory of the city of Zagreb. *Studia Geophysica et Geodaetica*, 53(1):17–38, doi:10.1007/s11200-009-0002-1.

Hofmann-Wellenhof, B. and Moritz, H. (2006). *Physical geodesy*. Springer Science & Business Media.

Jordan, S. K. (1972). Self-consistent statistical models for the gravity anomaly, vertical deflections, and undulation of the geoid. *Journal of Geophysical Research*, 77(20):3660–3670, doi:10.1029/JB077i020p03660.

Kaloop, M. R., Pijush, S., Rabah, M., Al-Ajami, H., Hu, J. W., and Zaki, A. (2021). Improving accuracy of local geoid model using machine learning approaches and residuals of GPS/levelling geoid height. *Survey Review*, pages 1–14, doi:10.1080/00396265.2021.1970918.

Kim, S.-K., Park, J., Gillins, D., and Dennis, M. (2018). On determining orthometric heights from a corrector surface model based on leveling observations, GNSS, and a geoid model. *Journal of Applied Geodesy*, 12(4):323–333, doi:10.1515/jag-2018-0014.

Ligas, M. (2022). Comparison of kriging and least-squares collocation–revisited. *Journal of Applied Geodesy*, 16(3):217–227, doi:10.1515/jag-2021-0032.

Ligas, M. and Szombara, S. (2018). Geostatistical prediction of a local geometric geoid-kriging and cokriging with the use of EGM2008 geopotential model. *Studia Geophysica et Geodaetica*, 62(2):187–205, doi:10.1007/s11200-017-0713-7.

Meier, S. (1981). Planar geodetic covariance functions. *Reviews of geophysics*, 19(4):673–686, doi:10.1029/RG019i004p00673.

Moritz, H. (1972). *Advanced least-squares methods*, volume 175. Ohio State University Research Foundation Columbus, OH, USA.

Orejuela, I. P., González, C. L., Guerra, X. B., Mora, E. C., and Toulkeridis, T. (2021). Geoid undulation modeling through the Cokriging method–A case study of Guayaquil, Ecuador. *Geodesy and Geodynamics*, 12(5):356–367, doi:10.1016/j.geog.2021.04.004.

Radanović, M. and Bašić, T. (2018). Accuracy assessment and comparison of interpolation methods on geoid models. *Geodetski Vestnik*, 62(1):68–78, doi:10.15292/geodetski-vestnik.2018.01.68-78.

Schaffrin, B. (2001). Equivalent systems for various forms of kriging, including least-squares collocation. *Zeitschrift für Vermessungswesen*, 126(2):87–93.

Tusat, E. and Mikailsoy, F. (2018). An investigation of the criteria used to select the polynomial models employed in local GNSS/leveling geoid determination studies. *Arabian journal of geosciences*, 11(24):1–15, doi:10.1007/s12517-018-4176-0.

Wackernagel, H. (2003). *Multivariate geostatistics: an introduction with applications*. Springer Science & Business Media, doi:10.1007/978-3-662-05294-5.

You, R.-J. (2006). Local geoid improvement using GPS and leveling data: case study. *Journal of Surveying Engineering*, 132(3):101–107, doi:10.1061/(ASCE)0733-9453(2006)132:3(101).

Zhong, D. (1997). Robust estimation and optimal selection of polynomial parameters for the interpolation of GPS geoid heights. *Journal of Geodesy*, 71(9):552–561, doi:10.1007/s001900050123.